

Numerical Investigation of the Flow Past 6:1 Prolate Spheroid

M. B. Subrahmanya * B.N.Rajani

Scientist, CTFD Division, CSIR-NAL, Bangalore 560 017, India

Abstract

The main objective of the present work is to simulate numerically the three-dimensional flow past a 6 :1 prolate spheroid at $Re = 4.2 \times 10^6$ for which extensive measurement data are available. The computations have been carried out using the in-house multi-block structured incompressible flow solution code 3D-PURLES and the effect of turbulence is simulated using Spalart Allmaras(SA) model and vorticity based Shear Stress Transport model (SST-V) model. The relative performance of these turbulence models have been assessed by comparing against the measurement data. The computations could capture the primary and secondary lines which matches fairly well with the measurements. The SST-V turbulence model predictions of the primary and secondary separation lines as well as the aerodynamic coefficients were better than that of SA turbulence model.

Keywords: turbulence models, separation line, pressure based incompressible solver, finite volume method.

1 Introduction

The three-dimensional flow separation is one of the most interesting and challenging problems in fluid mechanics. The complex flow structures observed behind the three dimensional bodies is a manifestation of flow separation and it is important to understand and predict these features. In spite of continuous research to understand three-dimensional flows, the physics of separation and the process of transition is not yet fully understood. The non-availability of accurate models for highly separated turbulent flows forms a stumbling block for accurate prediction using the CFD tools. Prolate spheroids are three-dimensional bodies having different aspect ratios which may be considered as simplified models of submarines, unmanned underwater vehicles, missiles, airships *etc.* Prolate spheroids though geometrically simple the flow characteristics are dominated by complex flow phenomenon like separation and transition. The primary focus of this work is to assess the capability of the turbulence models to capture the three-dimensional flow features of 6:1 prolate spheroid at different angles of attack (aoa) using the in-house multi-block structured incompressible flow solution code 3D-PURLES (**3D**-Pressure based **URANS** and **LES** solver) [7, 8]. In order to enhance the numerical stability, the original SST turbulence model of Menter [6] is modified to vorticity based model (SST-V) [1, 9, 12] and the SA model [11] is modified to prevent negative vorticity [5, 12].

2 Results and Discussion

Turbulent flow simulations are carried out for 6:1 prolate spheroid at $Re = 4.2 \times 10^6$ for different angles of attack using the SST-V and SA turbulence models. The computations use the central difference scheme (CDS) with deferred correction [3] for spatial discretization on a O-O grid topology with $111 \times 101 \times 264$ grid nodes and having a near wall resolution of $y^+ < 1$. The grid and boundary conditions used for the present simulations are shown in Fig. 1. The free stream turbulence energy (k) is maintained at 0.03% [2, 13] of the mean kinetic

*Corresponding author. Email: subrahmanya@nal.res.in

energy whereas the specific dissipation rate (ω) is prescribed assuming the local eddy viscosity (μ_t) to be approximately equal to the laminar viscosity (μ) and $\tilde{\nu}$ is assumed to be equal to the laminar kinematic viscosity (μ/ρ). The azimuthal variation of the surface pressure (C_p) and skin friction (C_f) coefficients at one axial location for

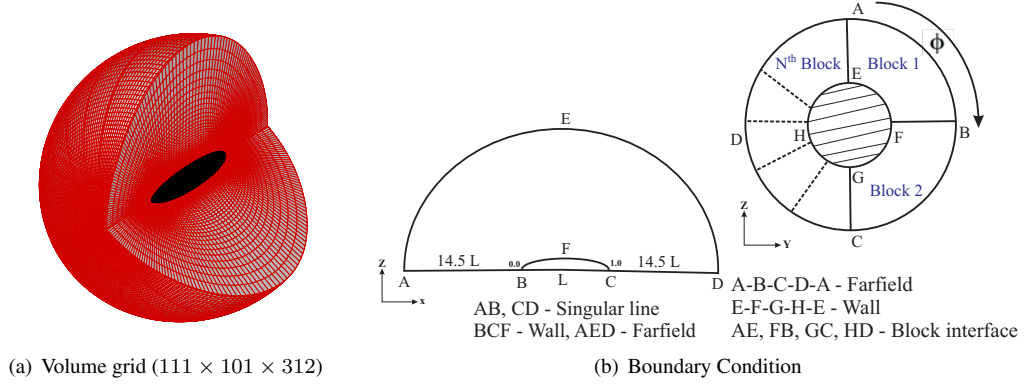


Figure 1: Grid and boundary condition used for flow past prolate spheroid

$\alpha = 30^\circ$ is shown in Fig. 2. The C_p predicted by both the models are almost identical, however some difference in C_f plot is observed especially in the windward region ($180^\circ \leq \phi \leq 250^\circ$) and the difference reduces as we approach the leeward side ($250^\circ \leq \phi \leq 360^\circ$). Kotapati-Apparao *et al.* [4] in their DES computations also reported a similar discrepancy and attributed it to the measurement errors as near the attachment line on the windward side a high C_f is not expected and hence unphysical. The separation line at different angles of attack is

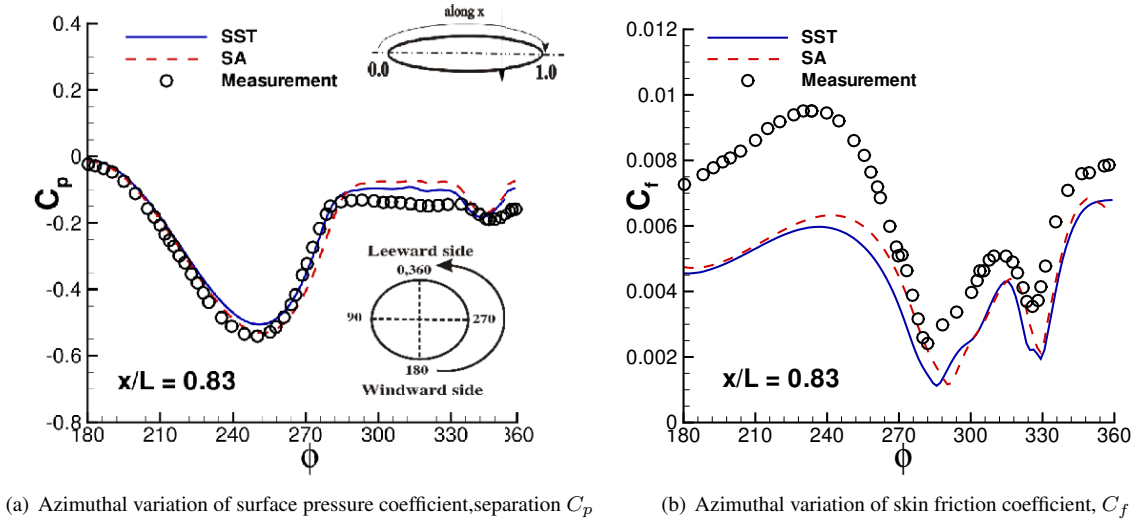


Figure 2: Effect of turbulence model for $\alpha = 30^\circ$
(Symbol - Measurement [13])

obtained using the minimum C_f criteria at different axial locations (X/L) as suggested by Sipmon [10, 13]. Similar to the experiments of Wetzel and Simpson [13] no separation line was observed below 10° angle of attack and secondary separation was observed only for $\alpha \geq 15^\circ$. The computed separation lines from 10° to 30° along with

the measurement [13] are shown in Fig. 3. The turbulence models have captured the measurement trend for both primary and secondary separation. The length of the primary separation line is in general over predicted whereas the onset of the separation is observed to occur early along the axial direction and delayed along the azimuthal direction. However this difference narrows down as the angle of attack increases (Fig. 3(c) and Fig. 3(d)) with SST model prediction being more closer to the measurement data. On the other hand, the length of the secondary separation line is under predicted and the onset is delayed in both the directions (axial and azimuthal). Similar to the primary separation a better match with the measurement is observed at higher angles of attack with SST model being slightly closer. The flow is expected to become fully turbulent at higher angles of attack and the SA and SST models which assume the flow to be fully turbulent have hence performed better at at higher angles of attack. The use of transition models like the $\gamma-Re_{\theta}$ model may improve the results at lower angles of attack. The

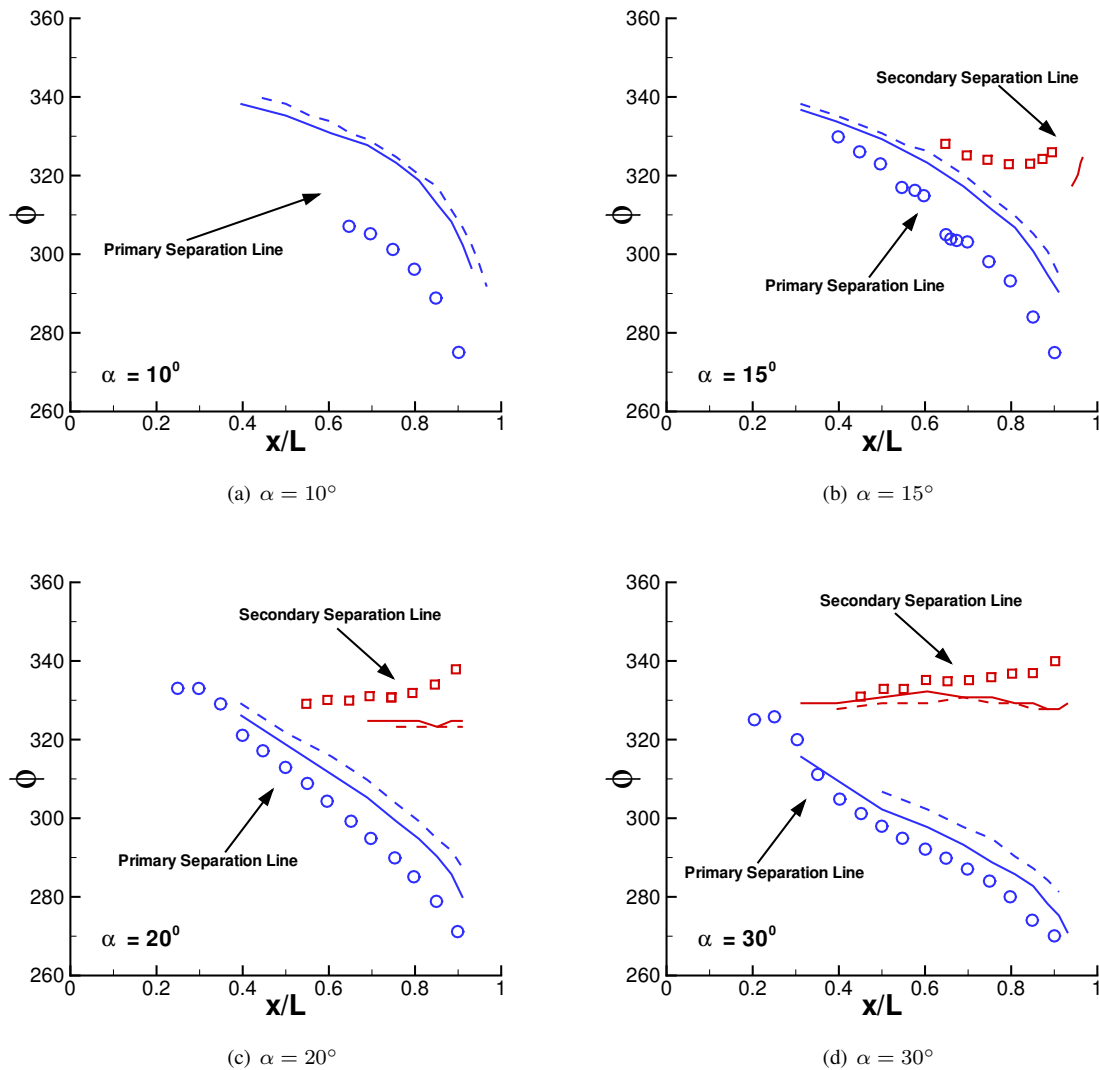


Figure 3: Comparison of the Separation lines at different angles of attack
Solid line - SST Model, Dashed line - SA Model, Symbol - Measurement [13]

typical surface streamlines at higher angles of attack (20° and 30°) obtained using the SST turbulence model are

shown in Fig. 4 where the separation line is indicated by converging lines. The first set of converging line towards the windward line of symmetry marks the primary separation and for 20° it is observed to initiate at $X/L \approx 0.4$ whereas for 30° it initiates slightly upstream ($X/L \approx 0.3$). The secondary separation which is designated by the second set of converging line is observed to be shifted towards the windward line of symmetry for both the angles of attack. The secondary separation line for 20° is observed to start quite downstream ($X/L \approx 0.7$). However for 30° the X/L location at which the secondary separation starts is quite similar to the primary separation. The onset of primary and secondary separation indicated by the surface streamlines corroborates with the separation line plot obtained by minimum C_f criteria. The C_f contours in Fig. 5 also show two regions of minimum C_f ; one towards the windward and other towards leeward corresponding to the primary and secondary separation lines respectively. The vorticity contour on the cross planes (Fig. 5) for the two angles of attack is observed to grow with its strength being higher for 30° .

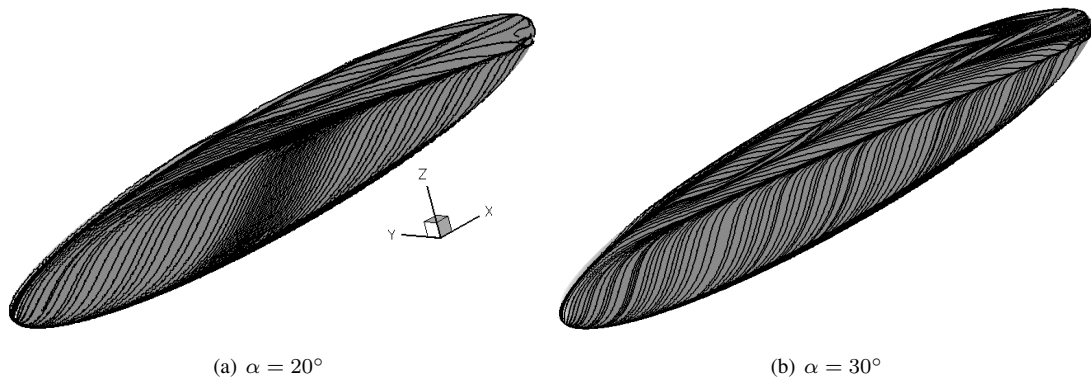


Figure 4: Surface streamlines obtained by SST turbulence model

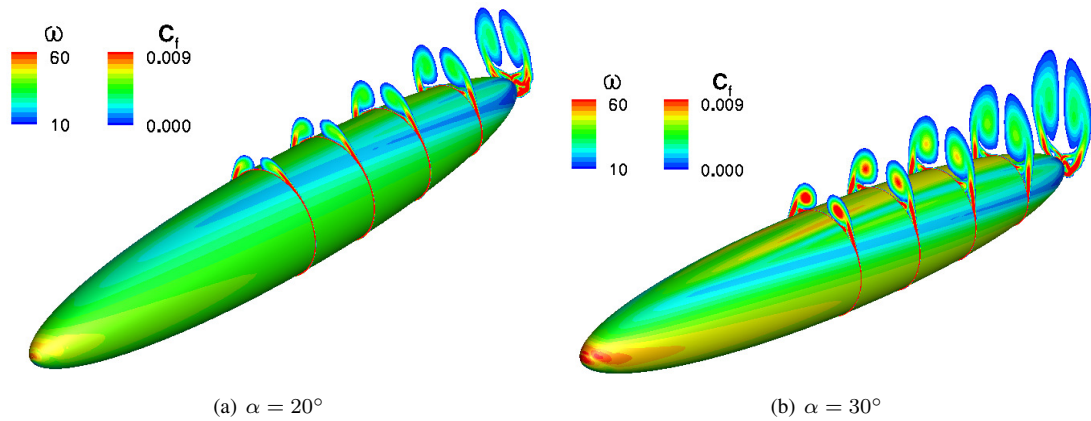


Figure 5: Contours of surface skin friction coefficient and vorticity magnitude at six cross planes for SST turbulence model

The comparison of normal force coefficient (C_Z) and moment coefficient (C_{MY}) obtained by the two turbulence models with measurement data [13] are shown in Fig. 6 and a reasonably good match is observed. It is further evident from this figure that the SST turbulence model is found to be in better agreement with measurement when compared to the SA model especially at higher angles of attack.

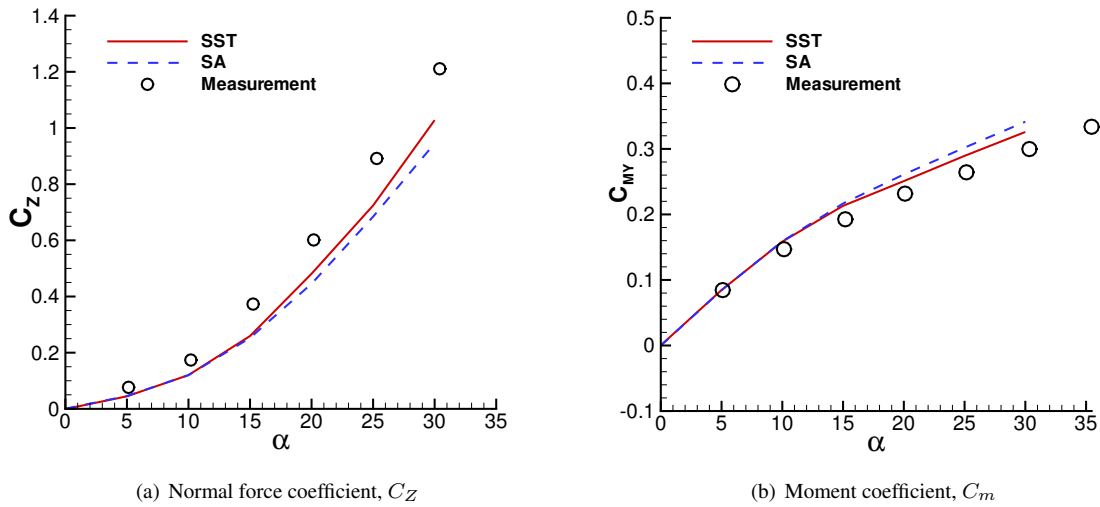


Figure 6: Aerodynamic coefficients (Measurement [13])

3 Concluding Remarks

Three dimensional separated flow over a 6:1 prolate spheroid at $Re = 4.2 \times 10^6$ has been simulated at different angles of attack ($0^\circ \leq \alpha \leq 30^\circ$) using SST and SA turbulence models available in 3D-PURLES. These turbulence models have been suitably modified by including limiters for the production term in both the models. The pressure coefficient distributions are in reasonably good agreement with the measurement data. On the other hand, the azimuthal variation of the skin friction coefficient was under predicted especially in the windward side similar to the DES computations of Kotapati-Apparao *et. al.* [4]. The primary and secondary separation lines on the leeward side predicted by the models at different angles of attack are similar to the measurements with SST being more closer. At higher angles of attack ($\alpha > 15^\circ$) the predicted separation lines are in better agreement with the measurements since the flow tends to become fully turbulent. Using transition models like the $\gamma-Re_\theta$ may improve the prediction of the separation line at lower angles of attack.

References

- [1] S. R. Allmaras, T. Johnson, and P. R. Spalart. Modification and clarification for the implementation of Spalart-Allmaras turbulence model. In *7th International Conference on Computational Fluid Dynamics (ICCFD7), Big Island, Hawaii, ICCFD-1902*, pages 1–11, July 2012.
- [2] C. J. Chesnakas and R. L. Simpson. Detailed investigation of the three-dimensional separation about a 6 : 1 prolate spheroid. *American Institute of Aeronautics and Astronautics Journal*, 35(6):990–999, 1997.
- [3] P. K. Khosla and S. G. Rubin. A diagonally dominant second-order accurate implicit scheme. *Computers and Fluids*, 2:207–209, 1974.
- [4] R. B. Kotapati-Apparao, K. D. Squires, and J. R. Forsythe. Prediction of a Prolate Spheroid Undergoing a Pitchup Maneuver. *AIAA Paper*, 2003-02-69:1–11, 2003.
- [5] F. R. Menter. Improved two-equation $k - \omega$ turbulence models for aerodynamics flows. Technical Report TM 103975, NASA, October 1992.

- [6] F. R. Menter. Two-equation eddy-viscosity turbulence models for engineering applications. *AIAA Journal*, 32(8):1598–1605, 1994.
- [7] B. N. Rajani and S. Majumdar. Numerical simulation of turbulent flow past a circular cylinder. Technical Report NAL PD CF 0805, National Aerospace Laboratories, Bangalore, 2008.
- [8] B. N. Rajani and S. Majumdar. Large Eddy Simulation of flow past circular cylinder in the lower subcritical regime ($Re = 3900$). Technical Report NAL PD CF 1004, National Aerospace Laboratories, Bangalore, 2010.
- [9] C. L. Rumsey, B. R. Smith, and G. P. Huang. Description of a website resource for turbulence model verification and validation. Technical Report Data Report VPI-AOE-20, Dept. of Aero & Ocean Engr, VPI & SU, Blacksburg, VA, 2010.
- [10] R. L. Simpson. Three-Dimensional Turbulent Boundary Layers and Separation. AIAA-95-0226, Reno, NV, 1995. 33rd Aerospace Sciences Meeting and Exhibit.
- [11] P. R. Spalart and S. R. Allamaras. A one-equation turbulence model for aerodynamic flows. *AIAA paper*, 92-0439, January 1992.
- [12] M. B. Subrahmanya and B. N. Rajani. Turbulent flow simulations of a 6:1 prolate spheroid. Technical Report PD-CTFD/2017/1015, National Aerospace Laboratories, Bangalore, 2017.
- [13] T. G. Wetzel and R. L. Simpson. Unsteady Flow Over a 6:1 Prolate Spheroid. Technical Report Report VPI-AOE-232, Advanced Research Projects Agency, 3701 Fairfax Suite 100, Arlington, VA, 1996.